Damage Detection in Thick-Walled Composites Using Surface Mounted Piezoelectric Elements

Final Report

July 15, 1997
Contract DAAD05-97-P0207

Prepared by:

Strategic University Resources
541 West Short Street/35
Lexington, KY 40507

Prepared For:

Aberdeen Test Center
STEAC-TS-PM
Aberdeen Proving Ground, MD 21005-5059

OK for public release

EXECUTIVE SUMMARY

The goal of the Phase 1 SBIR project described in this report was to develop a free vibration method for nondestructive evaluation of thick-walled composites. The governing principle of the free vibration method is that the frequency spectrum generated by a given object has the specificity of a fingerprint. Accordingly, if the boundary conditions, material properties, or geometry of the object are changed, some or all of the natural frequencies will change. Dramatic shifts have been observed in the natural vibrational frequencies of thin composite plates with the introduction of delaminations or other interply modifications; these observations provided the motivation for the present project in which the method was extended to thick plates.

In our version of the free vibration method, the composite is excited into vibration by a single mechanical pulse and the vibrational behavior is monitored by removable surface-bonded piezoelectric polymer film elements. When bonded to the surface of the composite, the piezoelectric film acts like a strain gage, except that it requires no external power source and generates signals far greater than those of a traditional amplified strain gage. The great sensitivity of the piezoelectric polymer film sensors and the simplicity of the overall test configuration makes this version of the method attractive for in-plant or in-field nondestructive evaluation.

After optimizing the details of the test configuration and demonstrating its ability to produce reliable frequency spectra, we proceeded to determine the level of internal damage needed to produce significant, damage-correlated changes in the frequency spectra of thick composite plates. This was done both experimentally, by acquisition of spectra for plates with and without delaminations, and also computationally, by frequency analysis of plates modelled with and without delaminations.

The major finding was that small to medium sized midplane delaminations in unidirectional thick plates *did not bring about the systematic frequency shifts* as documented in the literature for unidirectional thin plates in the frequency range 0-4000 Hz. Finite element computations confirmed the results found experimentally. Further experimental work on thick quasi-isotropic plates revealed that a delamination only began to produce noticeable frequency shifts when its area was nearly half that of the plate and when its free surfaces experienced negligible frictional interaction with each other.

The geometric aspect of a plate that determines natural vibrational frequencies is relative dimension, such as length-to-thickness, not absolute dimension, such as thickness alone. Therefore, the findings in this report best describe thick composite structures whose length-to-thickness ratios are in the range 20-30. For delaminations to have a greater effect, the length-to-thickness ratio would have to increase (a longer, less thick composite). Since the free vibration method as described in this report is not sensitive enough to identify small to medium delaminations in thick plates, we are not soliciting Phase 2 funding.

TABLE OF CONTENTS

INTRODUCTION

The residual stress that develops in thick-walled composite structures during fabrication can be high - much higher than in thin-walled structures. High residual stress has the possibility of producing internal damage, such as delamination and matrix cracking, before the structure is subjected to any applied load whatsoever. Such internal damage is not detectable by visual inspection. If internal cracks are large enough thay can lead to early catastrophic failure of the composite; small internal cracks can grow slowly under load until they are large enough to cause failure. Furthermore, cracks or delaminations that are too small to cause immediate failure can still reduce some aspects of mechanical performance of the composite [1-12].

Because of the potential of internal damage to produce lowered performance or early failure, it is important that it be detected before the composite is put into service. It would also be beneficial to be able to detect the formation of new internal damage at any time during the service life of the composite. Any practical method for detecting damage in the plant or field must be not only nondestructive but also sufficiently sensitive to reveal small localized damage buried deep within thick composites.

Nondestructive evaluation of composite structures for internal damage is not new. However, existing methods have various drawbacks that make them impractical for real-time, 100% inspection. For example, the well-established ultrasonic C-scanning method is extremely time-consuming because it uses a point probe that needs to be moved in small increments over the whole surface of the structure. Another example, infrared thermography [13], requires inconvenient differential heating of the structure. Other methods, such as vibrothermography [14], are not yet well developed and must be conducted and interpreted in the laboratory by experts.

The nondestructive evaluation method described in this report can be applied in a rapid and simple manner. It is a free vibration method, where the governing principle is that a given object has very specific vibrational behavior. In fact, the frequency spectrum

generated by a given object has the specificity of a fingerprint. However, some or all of the natural frequencies will change when the boundary conditions, material properties, or geometry of the object are changed. Dramatic shifts were observed in the natural vibrational frequencies of thin composite plates and beams when delaminations or other interply modifications were introduced [15-21]. These observations provided the motivation for our attempting to apply the method to thick plates.

The free vibration method requires only a pulse to excite the object of interest into vibration and a device to sense the vibrational response of the object for a designated time period. The excitation must be easy to apply and should involve forces too small to damage the composite or change its natural vibrational behavior. The sensing device must be easy to apply and remove from the composite surface and must be extremely sensitive to low-amplitude vibrations. Obviously, the simpler and more straightforward are the excitation and sensing devices, the more practical will be the free vibration method.

Our version of the free vibration method has removable surface-bonded piezoelectric polymer film elements as sensors to monitor the vibrational behavior of the composite structure. When bonded to the surface of the composite, the piezoelectric film acts like a strain gage, except that it requires no external power source and generates signals far greater than those of a traditional amplified strain gage [21-23]. Electrically, the piezoelectric film sensor behaves like a strain-dependent voltage source, extending and retracting as the plate vibrates, delivering a signal in the form of a cyclic voltage to the computer.

In our method, shown schematically in Figure 1, the composite plate is excited mechanically into free vibration by a light tap, and the signals from the piezoelectric sensors are converted from the time domain to the frequency domain by a fast Fourier transform. The result is a vibrational frequency spectrum, such as is shown in Figure 2.

It must be emphasized that the free vibration method, as applied in the work reported

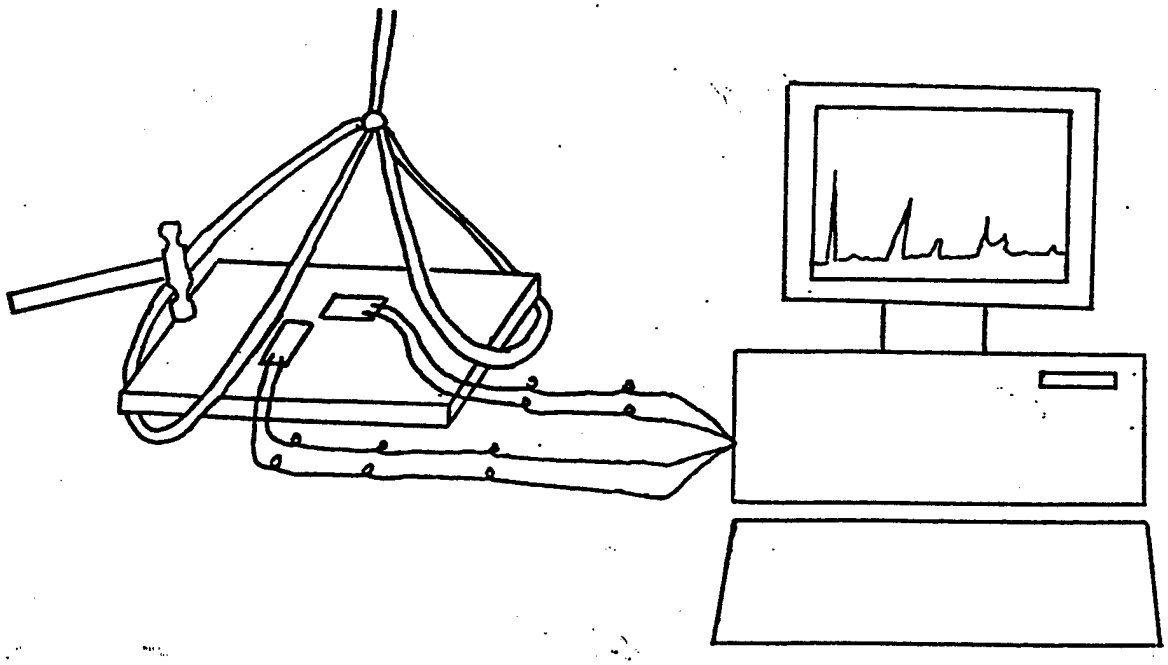

Figure 1. Experimental Set-Up for Free Vibration Testing. Plate is excited into vibration by a hammer tap. Piezoelectric sensors bonded to plate surface pick up signal and transit signal to computer, which displays a frequency spectrum.

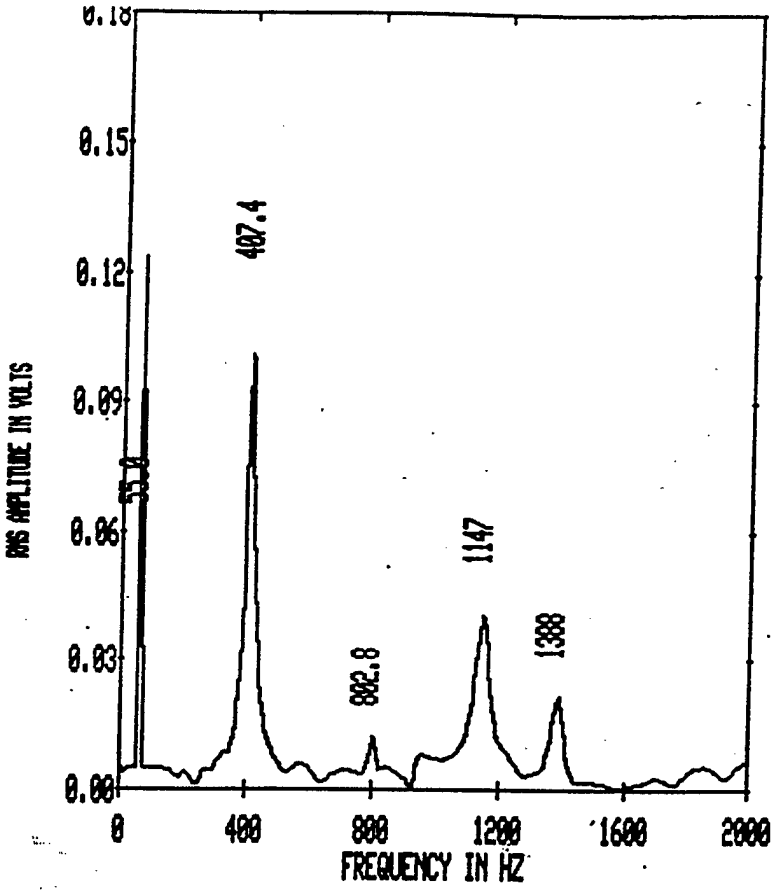

Figure 2. Vibrational Frequency Spectrum of Unidirectional Composite Plate. Amplitude in volts is plotted against frequency in Hz. This particulat spectrum was collected by a piezoelectric patch oriented at 90° to the fiber axis.

here, has the potential to indicate the presence and relative size of internal damage, but not to pin-point its location. In previous work, the method was applied successfully to thin plates (0.047 inches thick), where midplane delaminations as small as 0.34% of the plate area were detected [21]. For thick plates, which are much stiffer, the primary issue is the minimum size or severity of internal damage that will produce observable shifts in the natural frequencies.

PROJECT GOAL

The goal of this project, Phase 1 of an SBIR award, was to develop the free vibration method for nondestructive evaluation of thick-walled composites. Meeting this goal required 1) determining the optimum support, excitation, and sensor configurations for collection of frequency spectra, 2) establishing the random variation inherent to the method itself, 3) determining the level of internal damage needed to produce significant, damage-correlated spectral changes, and 4) distilling the findings into useful rules for application of the method. The remainder of this report describes how the goal was pursued and presents the results.

EXPERIMENTAL PROCEDURES

Prepreg preparation

Glass fiber/epoxy prepreg was made on a drum winder from S2 glass roving (Owens Corning Fiberglas, Toledo, OH) sized with epoxy-compatible coupling agent. The epoxy resin system was a stoichiometric mixture of diglycidyl ether of bisphenol A (Epon 828, Shell Chemical, Houston, TX) and the amine curing agent 1,3-phenylene diamine (Aldrich, Minneapolis, MN). The resin content of the prepreg was determined by mass difference before and after solvent extraction of a specimens cut from each tape.

Lay-up

Plies were cut to measure from chilled, uncured prepreg and were carefully stacked one-by-one in a steel picture frame mold to which a spray-on release agent had previously been applied. Care was taken to keep the fiber properly aligned with respect to a reference axis and to manually displace air with a roller as each ply was placed on the stack. For each controlled delamination, a circle or square of Kapton polyimide release film (Du Pont, Wilmington, DE) was placed between plies at the desired location.

Lamination

Each lay-up was laminated by the vacuum bag-autoclave method as follows. The lay-up, situated in the picture frame mold, was placed in the autoclave. A temperature-resistant rubber sheet was placed on top of the lay-up to form a vacuum bag and a 15-psi vacuum was pulled. After the autoclave was closed, the outside of the vacuum bag pressurized with N_2 to 80 psi and was held at room temperature for 30 min. to "debulk" the lay-up. The purpose of the debulking was to remove as much air and volatile matter before the start of heating. After debulking, the vacuum and pressure were maintained, and the lay-up was cured by a three-hour temperature ramp from 25°C to 120°C (77°F - 250°F), followed by a one-hour hold at 120°C. The cured composite was allowed to cool slowly

in the autoclave and was removed from the picture frame mold at room temperature.

Static characterization of laminated plates

Fiber volume was computed from prepreg resin content values, since little to no resin bleed-out occurred during lamination. Where possible, i.e., when the original plates were cut into smaller plates or sectioned, fiber volume fraction was verified by the resin burn-off method (15 h in muffle furnace at 600°C). Resin burn-off results from laminates were in excellent agreement with prepreg solvent extraction results. Thickness measurements for each laminate were made from edges to center with a deep-throated micrometer. A qualitative evaluation of resin distribution and void content associated with our fabrication methods was obtained by microscopy on samples cut from one of the laminated plates. A Krautkramer Branson USN50 (Lewistown, PA) portable ultrasonic flaw detector was used to examine plates containing the controlled delaminations made from embedded Kapton film. This flaw detector operates in a pulse-echo mode. The hand-held transducer was coupled to the top surface of the composite plate with Windex, and was moved slowly along the surface in a regular pattern while the display was monitored for echoes from the delaminations.

Plate support configurations for vibration testing

For the edge-clamped (cantilever plate, or fixed-free-free-free) configuration, the unheated platens of a laboratory press were used to grip one edge of the composite plate to be tested (Figure 3, top). The edge of the plate was slipped between the platens to a depth of 1 inch (25.4 mm). A piece of plywood of the approximate thickness of the composite plate was placed in the remaining gap between the platens for prevention of nonparallel closure. Cardboard shims were used as needed to equalize the composite plate and plywood thicknesses prior to press closure. Unidirectional plates were always edge-clamped so that the fiber direction pointed into the press. Both a Wabash automatic hydraulic press and a Carver manual hydraulic press were tried initially, but the automatic hydraulic press was disqualified because it introduced spurious peaks to

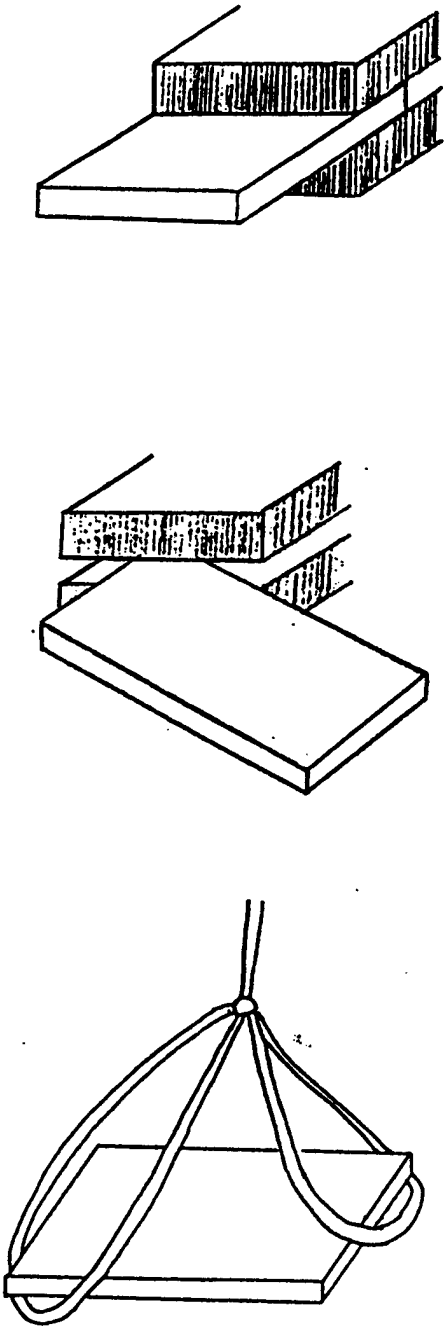

Figure 3. Plate Support Configurations for Free Vibration Testing. The edge-clamped (top), corner-clamped (center), and unsupported (bottom) configurations are shown. Each configuration imposes different boundary conditions on the plate, thereby resulting in a different spectrum.

the spectrum.

For the corner-clamped configuration, the Carver manual hydraulic press was used. A piece of plywood with a 90° notch cut in one edge was used as a fixture for reproducible placement of the plate corner in the press (Figure 3, center). The plywood also served to fill the gap when the platens were closed on the corner of the test plate. Cardboard shims were also used here to equalize the composite plate and plywood thicknesses. Trials were made with different amounts of the composite plate clamped in the platens.

The unsupported (free-free-free-free) configuration was closely approximated by suspension of the plate from the ceiling in a sling made of rubber tubing (Figure 3, bottom). The mass of the tubing relative to that of the plates was extremely small, as was the stiffness of the tubing relative to any of the plate stiffnesses. Based on these two conditions, the influence of the sling on the natural frequencies was assumed to be negligible.

Sensors and signal processing for vibration testing

Poled, electroded polyvinylidene fluoride (PVDF) film elements from AMP Inc. (Norristown, PA) were used as sensors. The relevant mechanical and piezoelectric properties of the polyvinylidene fluoride (PVDF) film are presented in Table 1 [24]. Each sensor, with an active area of 12 mm x 30 mm (0.47 in. x 1.2 in.), was bonded to the plate surface by means of double-backed cellophane tape. Since the stiffness of the PVDF film (see Table 1) was at least five times lower than the lowest stiffness of the composite, the sensors were elastically compatible in all directions with the surface of the composite. The PDVF film sensor was made part of a circuit by means of polymer-coated stainless steel wire (Cooner Wire Co., Chatsworth, CA), manufactured for use in cardiac pacemaker applications. The end of each wire was stripped free of polymer coating and held in contact with the metal surface of the sensor by a small piece of electrical tape.

Table 1. Relevant Mechanical and Piezoelectric Properties for PVDF Film Sensors [24].

Young's Modulus, E	2.5 GPa
Piezo-Strain Constants	
d_{31}	23×10^{-12} m/V
d_{32}	3×10^{-12} m/V
d_{33}	-33×10^{-12} m/V

Data from the analog signal coming from each piezoelectric sensor was captured at high speed by a personal computer outfitted with WAVEPAK integrated hardware and software (Computational Systems, Inc., Knoxville, TN). The WAVEPAK software allowed the personal computer to function as a multi-channel fast Fourier transform signal analyzer and to produce and display a frequency spectrum from each sensor coupled to the vibrating plate.

Each stored (disc or print-out) spectrum was the average of five free vibration tests, performed in immediate succession and electronically averaged. Print-outs of the frequency spectra were compiled in a three-ring binder. Typically, we collected and stored several spectra from each plate in a given support configuration. This allowed us to further average the results, yielding the average frequencies and standard deviations shown in the frequency tables presented in this report.

Computational modelling of free vibration

The computational model used for vibrational frequency analysis was based on the eight-node solid element with incompatible bending modes, as developed by Wilson and Ibrahimbegovic [25]. This element is available in the commercial computer code SAP2000N,

V6.02 [26]. An initial analysis was run to verify that SAP2000N would produce the same results obtained by Jian *et al* [21] with the commercial ANSYS computer code. The frequency analysis results matched.

A frequency analysis was then conducted for unidirectional, rectangular plates, in the cantilever plate configuration. Properties, dimensions, and midplane delaminations were chosen to correspond to experimental composite plates No. 3-6-97-0, No. 3-6-97-2, and No. 3-7-97-3, which had no, 2-in., and 3-in. delaminations, respectively. Representative properties for a unidirectional glass-epoxy composite at 50% fiber volume were taken from the literature [27] and are shown in Table 2 below. Plate dimensions used were 9.80 in. x 5.20 in. x 0.388 in., with the 5.2-in. edge held fixed. An 18 x 10 mesh of elements was used to discretize the plate; elements were 0.50-in. square, except along the edges where the dimensions were 0.30 in. to conform to the selected plate dimensions. Delaminations were modelled by double nodes at the free surfaces between lamina. No consideration of the delamination edge singularity was included in the finite element model.

Table 2. Material Properties for Unidirectional Glass-Epoxy Laminate of 50% Fiber Volume [27].

Longitudinal modulus, E_{11}	42.4 GPa
Transverse modulus, E_{22}	11.6 GPa
Longitudinal shear modulus, G_{12}	4.68 GPa
Longitudinal shear modulus, G_{13}	4.68 GPa
Transverse shear modulus, G_{23}	4.07 GPa
Major Poissons ratio, ν_{12}	0.305
Minor Poisson's ratio, ν_{21}	0.083
Transverse Poisson's ratio, ν_{23}	0.417
Mass density, ρ	1820 kg/m^3

EXPERIMENTAL RESULTS

Plate dimensions, fiber volumes, and ultrasonic flaw detection

Figure 4 contains diagrams of the unidirectional plates fabricated and lists their dimensions and fiber volumes. The delaminations were at the midplane and are indicated in the figure by dotted lines. Figure 4 also shows, by dotted lines, where the square plates were subsequently cut to form smaller, rectangular plates. (Detailed maps of thickness for the unidirectional plates are shown in Appendix A.) Only Plate No. 1-29-97 was sectioned for microscopy. A magnification of 800X showed that the plate had fairly uniform resin distribution and negligible void content.

Figure 5 contains diagrams of the quasi-isotropic plates fabricated and lists their dimensions and fiber volumes. (Detailed maps of thickness for the two quasi-isotropic plates are shown in Appendix A.) Each plate was 40 plies thick and had two 4-in. square delaminations located in the same quadrant of the plate. One delamination was between plies 6 and 7, and the other was between plies 10 and 11. The delaminations are indicated by dotted lines. Subsequent cutting lines are also shown in Figure 5.

All of the simulated delaminations depicted in Figures 4 and 5 were detected by the Krautkramer Branson USN50 portable ultrasonic flaw detector.

Optimization of sensor configuration

The term sensor configuration refers to the sensor's location on the plate surface and the sensor axis' orientation angle with respect to the plate geometric axis. The optimum sensor configuration was determined iteratively in conjunction with determination of support configuration and excitation details.

At first, sensor location over the surface of the test specimen was varied widely. However, it became evident early in the program that sensor location did not greatly

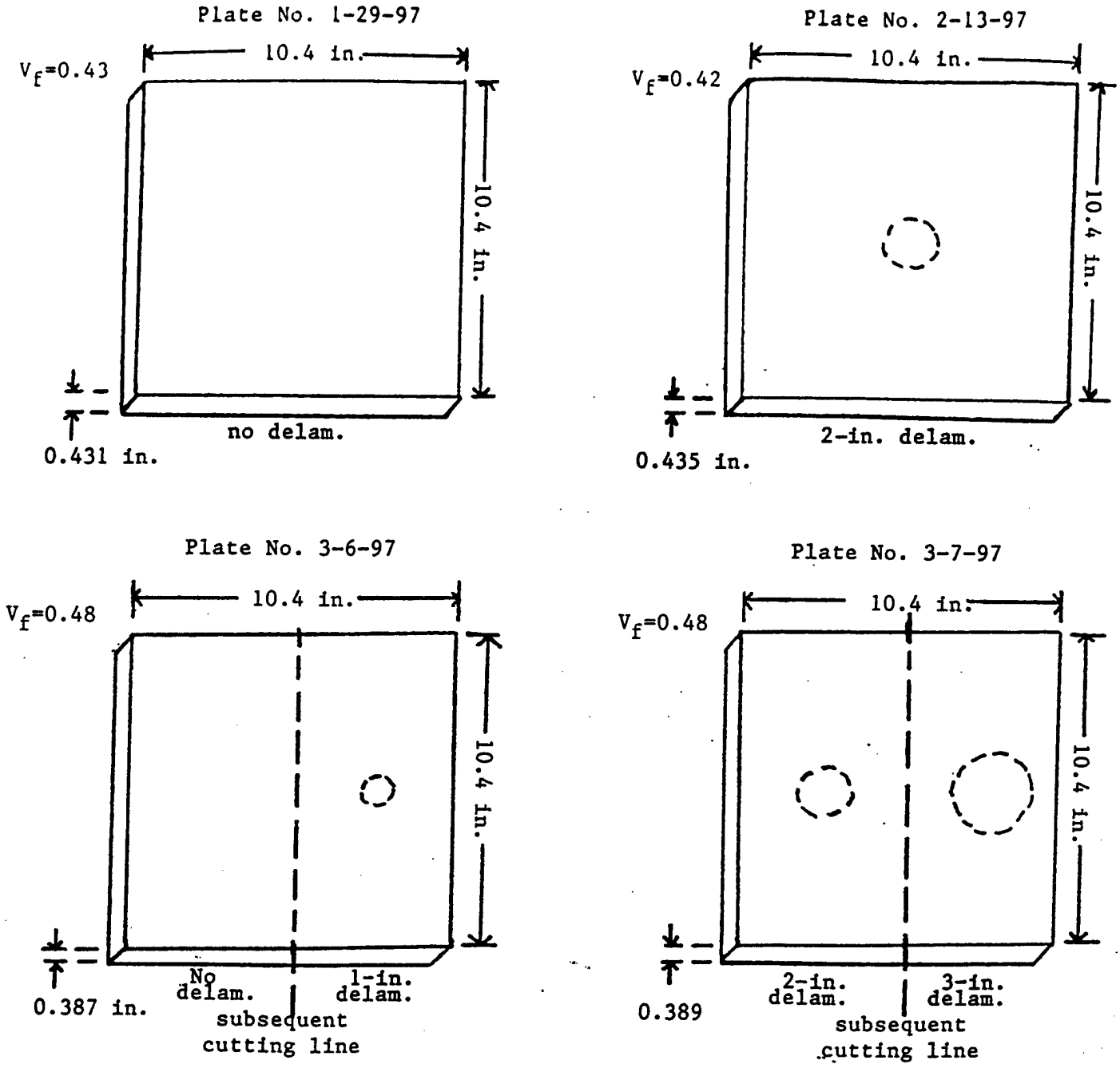

Figure 4. Diagrams of Unidirectional Plates Fabricated. Circular midplane delaminations are indicated by dotted lines. Also indicated by dotted lines are the lines along which the plates were subsequently cut to form narrower plates.

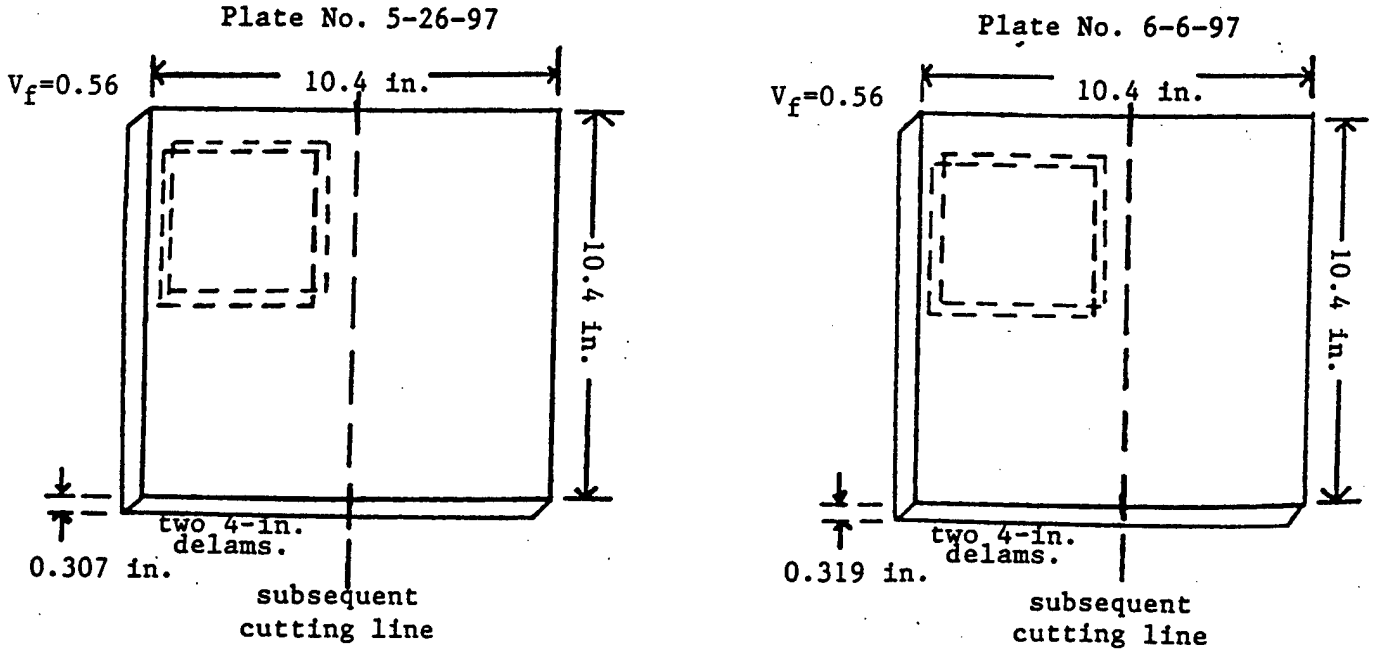

Figure 5. Diagrams of Quasi-Isotropic Plates Fabricated. Square delaminations are indicated by dotted lines. Two delaminations were placed in each 40-ply plate, between plies 6,7 and between plies 10,11. Each delamination in right hand plate was made from two Kapton films coated with mold release and stacked together. After test each plate was cut along dotted straight line Also indicated by dotted lines shown in figure to yield two narrower plates.

influence the amplitudes or the frequencies of the peaks in the vibrational spectrum. Even for edge-clamped plates, the difference between positioning the sensor close to the clamp and at the free edge opposite the clamp was quite small. Perhaps this spectral insensitivity to sensor location is reasonable in view of the fact that free vibration in a plate is a global property of the plate.

Sensor orientation, the angle between the sensor axis and the plate's geometric axis was also varied widely at first. Trial and error showed that for any selected location on the plate surface, parallel and perpendicular orientations were sufficient, and that other angular orientations gave no additional information. Besides being sufficient, the use of parallel and perpendicular sensors was also necessary. This was because some modes (frequencies) were captured by the parallel sensor, but weakly or not at all by the perpendicular sensor, and vice versa.

In sum, best results were achieved when the sensors were positioned on the plate surface as a pair at right angles to each other, i.e., parallel and perpendicular, respectively, to the edges of the plate. Use of frequency spectra from both sensors gave the most complete list of experimentally extracted frequencies of the vibrating plate.

Determination of support configuration

The goal was to identify the support configuration that allowed as many vibrational modes as possible to be excited in the plates, and that also had minimal adjustment and reproducibility problems. Of course, different support configurations resulted in different frequency spectra, even for the exact same test plate. This is shown in Figure 6, which presents spectra from Plate No. 3-7-97-3 in the edge-clamped (left), unsupported (center), and corner-clamped (right) configurations.

All three support configurations gave good readable spectra, with sufficient numbers of major peaks for a reliable characterization of the plate. The corner-clamped configuration was the most delicate and troublesome in terms of reproducibility. A thorough

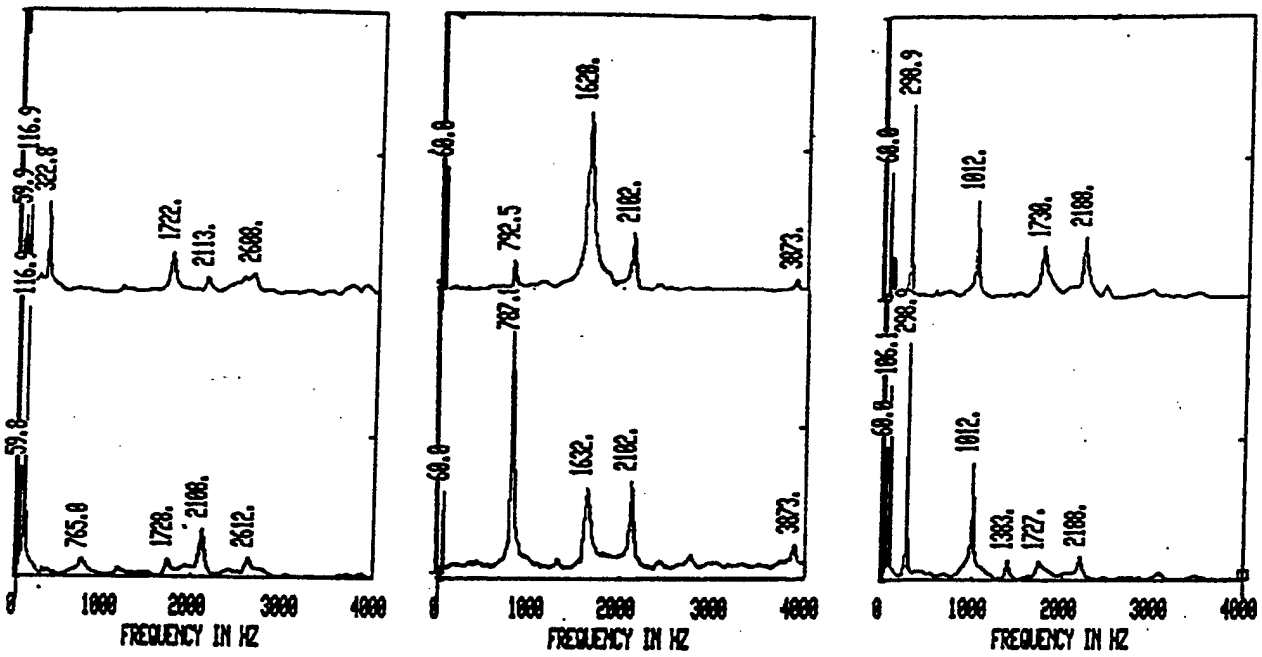

Figure 6. Comparison of Frequency Spectra Obtained with Different Support Configurations. Spectra of edge-clamped (left), unsupported (center), and corner-clamped (right) unidirectional plate with 3-in. midplane delamination are shown. Top spectrum in each set is from the 90° sensor; bottom spectrum is from 0° sensor.

comparison showed that spectra obtained in the corner-clamped configuration offered no advantage over the other configurations; therefore, corner-clamping was discontinued.

The edge-clamped configuration showed sensitivity to clamping pressure (frequencies shifted to slightly higher values as clamp pressure was increased), so care had to be taken to control clamping pressure to a known, reproducible value. In spite of this delicate aspect, we felt it was important to retain the edge-clamped configuration, because it is analogous to the well-studied cantilever plate geometry for which computational models are available.

The unsupported configuration was found to be just as fruitful as the edge-clamped configuration in terms of providing a spectrum. In terms of practicality, the unsupported configuration is superior, because the tester does not have to bother with devising procedures and methods for ensuring reproducible clamping.

In sum, because both unsupported and edge-clamped configurations were simple to set up and yielded good spectra, they were retained throughout the experimental program. The corner-clamped configuration, more difficult to set up and offering no advantage, was eliminated from further consideration.

Determination of excitation procedure

A single, light tap with a hand-held hammer worked surprisingly well, and was used as the instrument of excitation throughout this Phase I project. A forceful hit proved to be undesirable, since it transmitted an impulse to the massive press, whose reverberations caused a series of extra peaks to appear in the spectrum. Another procedure, mechanical springback (release from an imposed deformation), was tried and found to be more troublesome and no better than the simple hammer tap.

Different tap locations on the plate surface and plate edge were explored systematically. While surface and edge taps excited most of the same frequencies, surface taps gave

higher amplitudes for some frequencies while edge taps gave higher amplitudes for other frequencies. (Certain locations, e.g., too close to the clamped edge, were found to generate spectra with low amplitudes overall.) Taps both on and off the major geometric axis of the composite plate were able to excite torsional as well as bending vibrational modes. Once it was determined that excitation of (at least some) torsional modes was not a problem, all subsequent tests were done twice - once with a surface tap and once with an edge tap.

In sum, a review of all the spectra revealed that excitation by edge tap and by surface tap both excited the major frequencies, but tended to give complementary amplitudes.

Random variation associated with the free vibration method itself

The random variation inherent to the free vibration method is defined as the variation observed in repeated testing of a single plate, including removal and reapplication of sensors, as well as removal and replacement of the test plate in the support configuration. Collection of numerous spectra over a several-day period permitted a mean and standard deviation to be calculated for each peak in the spectrum.

All the subsequent tables in this report list the means and standard deviations for experimentally extracted peaks. Typical standard deviations were only a few Hz. Occasionally, however, standard deviations as high as 15 Hz were seen for some very weak peaks at high frequency. We felt that this variation arose from detection of what were probably closely spaced or double frequencies, where each frequency was detected by a different sensor, and the two were then averaged as though they were the same peak.

In sum, the random variation of the free vibration method itself, as evaluated on any given plate, was small. For most peaks, the coefficient of variation (1 std. dev./mean) was under 1%.

Experimental spectra for unidirectional thick plates with and without midplane delaminations

This section describes the findings for unidirectional thick plates with different-sized delaminations embedded at the midplane. The results for the quasi-isotropic plates are presented in a later section.

The major point to be made is that the presence of midplane delaminations did not produce the expected systematic downward shift in vibrational frequencies. This absence of effect is shown by three examples, the first of which is reported Table 3. Table 3 shows the major frequencies obtained from two similar plates, fabricated early in the project from two different batches of prepreg. Although Plate No. 2-13-97 contains a 2-in. midplane delamination, its frequencies do not show a systematic decrease with respect to those of Plate No. 1-29-97, which contains no midplane delamination. Since a delamination would tend to reduce frequencies and not increase them, the observed spectral differences between the plates must be deemed due to fabrication inconsistencies and independent of any delaminations.

The second example is shown in Table 4, which lists the major frequencies obtained from Plates No. 3-6-97 and 3-7-97. These plates were fabricated from the same batch of prepreg to equal dimensions and fiber volumes, but with different midplane delaminations (see Figure 4). The frequencies obtained from the two plates are remarkably similar. The delaminations appear to have had no effect on the vibrational behavior of the plate; that is, none of the frequencies of Plate No. 3-6-97 are shifted downward with respect to those of Plate No. 3-7-97.

The third example was constructed by cutting Plates No. 3-6-97 and 3-7-97 in half along the fiber direction (as depicted in Figure 4) to produce four rectangular plates. These rectangular plates formed a series of specimens that were equal in every way except for systematically increasing midplane delamination size. (It is useful to note that the midplane delaminations in these cut plates were larger with respect to plate area than in

Table 3. Plate-to-Plate Comparison for Unidirectional Plates Made from Different Prepreg Batches (Ave. Freq. ± 1 Std. Dev.)

Edge-clamped configuration:

Plate No. 1-29-97	Plate No. 2-13-97
130.4 ± 4.0	127.8 ± 0.3
206.5 ± 1.8	215.0 ± 1.6
232.3 ± 0.3	232.1 ± 0.3
516.3 ± 2.3	538.3 ± 2.9
807.5 ± 5.0	828.4 ± 3.4
960.4 ± 5.6	951.7 ± 2.1
1189 ± 2.7	1173 ± 0.0
1287 ± 8.9	1292 ± 3.1
1875 ± 2.0	1923 ± 5.8

Unsupported Configuration:

Plate No. 1-29-97	Plate No. 2-13-97
176.1 ± 3.18	207.7 ± 0.07
248.1 ± 1.98	255.7 ± 2.39
391.5 ± 1.76	406.9 ± 1.49
640.0 ± 4.27	667.5 ± 4.95
784.2 ± 2.30	804.2 ± 2.17
916.4 ± 4.15	943.1 ± 3.20
1098 ± 5.45	1145 ± 4.48
1305 ± 2.21	1360 ± 4.04
1342 ± 1.55	1389 ± 4.77

Table 4. Plate-to-Plate Comparison for Unidirectional Square Plates Made from a Single Prepreg Batch (Ave. Freq. ± 1 Std. Dev.)

Edge-clamped configuration:

Plate No. 3-6-97	Plate No. 3-7-97
117.9 ± 0.2	118.5 ± 1.1
207.4 ± 0.6	207.7 ± 0.3
226.7 ± 1.9	-
512.7 ± 0.1	514.8 ± 2.3
766.0 ± 2.2	781.6 ± 1.9
924.2 ± 11.6	928.6 ± 5.5
1181 ± 2.7	1180 ± 5.8
1247 ± 4.7	1262 ± 3.3
1867 ± 14.6	1883 ± 0.6

Unsupported Configuration:

Plate No. 3-6-97	Plate No. 3-7-97
-	163.8 ± 1.8
247.4 ± 2.4	247.6 ± 2.7
382.7 ± 0.2	382.7 ± 0.1
658.7 ± 1.8	657.4 ± 0.0
782.4 ± 0.2	789.6 ± 5.3
915.1 ± 4.9	926.3 ± 2.5
1097 ± 4.4	1093 ± 3.8
1347 ± 17.1	1345 ± 19.8

the original uncut plates.) Table 5 shows the frequencies obtained for all four rectangular plates in the series. The frequencies are remarkably similar and show no systematic changes as a function of increasing delamination size.

In sum, midplane delaminations in unidirectional thick plates did not cause the dramatic frequency shifts documented in the literature for unidirectional thin plates with midplane delaminations.

Results of frequency analysis by computational model

The lack of effect was disappointing, because it suggested that the free vibration method, so promising in thin plates, could not be extrapolated to thick plates. To understand the physical basis for the observed lack of effect, we conducted a frequency analysis by means of a finite element model. The next section presents the results of this modelling.

Table 6 presents the first twenty modal frequencies obtained from SAP2000N. Comparison of the column for no delamination with the column for a 2-in. square delamination reveals that a midplane delamination of medium size is predicted to have very little influence on frequency response. The typical frequency change with respect to the first column is less than 1%; the maximum frequency change is 4.4% (in mode 19). A similar pattern is observed when the delamination is increased to 3 in. square. For the twenty modes calculated, only modes 16, 19, and 20 exhibit frequency changes greater than 10%, with the maximum change being 21% (in mode 19). Unfortunately, in practice, these modes have frequencies outside the range attainable by our experimental apparatus.

Table 7 presents a direct comparison of the finite element (FE) results with the experimental results of Table 4. Since the effects of delamination on the first ten computed frequencies were small and on the corresponding experimental frequencies were imperceptible, the values from no delamination, 2-in. delamination, and 3-in. delamination were averaged for presentation in Table 7. Table 7 shows that the finite element and experimental frequency results compare very well for the first three fundamental modes.

Table 5. Plate-to-Plate Comparison for Unidirectional Rectangular Plates (Ave. Freq. ± 1 Std. Dev.)

Edge-clamped configuration:

Plate No. 3-6-97-0	Plate No. 3-6-97-1	Plate No. 3-7-97-2	Plate No. 3-7-97-3
113.4 ± 0.3	116.9 ± 0.8	117.8 ± 8.0	115.9 ± 1.7
317.0 ± 0.3	320.0 ± 2.3	299.9 ± 0.0	315.0 ± 13.1
743.7 ± 2.1	760.1 ± 3.5	794.0 ± 23.0	763.7 ± 1.8
1693 ± 0.5	1726 ± 4.9	1704 ± 17.5	1722 ± 4.7
2080 ± 2.8	2138 ± 0.0	2118 ± 0.0	2105 ± 6.6
2445 ± 2.7	2493 ± 0.0	2487 ± 26.2	2610 ± 2.8

Unsupported configuration:

Plate No. 3-6-97-0	Plate No. 3-6-97-1	Plate No. 3-7-97-2	Plate No. 3-7-97-3
775.0 ± 3.0	780.8 ± 3.0	790.9 ± 2.7	784.2 ± 3.1
1611 ± 2.2	1634 ± 2.4	1603 ± 0.5	1631 ± 2.0
2076 ± 3.2	2093 ± 0.5	2106 ± 2.0	2093 ± 15.6
3852 ± 0.6	3869 ± 2.3	3893 ± 0.6	3876 ± 3.5

Table 6. Finite Element Computed Frequencies for the Unidirectional Rectangular Composite Plate (Hz)

Mode	Computed Frequency delam. = 0 in	Computed Frequency delam. = 2 in	Computed Frequency delam. = 3 in
1	124.63	124.50	123.91
2	306.12	306.11	305.97
3	763.66	763.10	759.77
4	1094.16	1091.57	1082.25
5	1116.43	1116.43	1116.43
6	1493.00	1491.67	1479.99
7	2077.47	2046.00	1920.95
8	2180.98	2167.99	2120.81
9	2379.04	2376.37	2349.05
10	3368.29	3298.24	3153.98
11	3539.34	3539.34	3267.31
12	3727.52	3605.50	3539.34
13	3939.93	3916.30	3777.75
14	4149.50	4062.87	3947.72
15	4269.94	4197.16	4153.20
16	4849.46	4849.47	4183.03
17	5026.38	4997.08	4763.55
18	5194.58	5150.64	4849.48
19	6222.03	5953.04	4919.33
20	6397.87	6351.28	5516.43

Table 7. Comparison of Averaged Finite Element (FE) and Experimental Frequencies for Unidirectional Rectangular Composite Plates

FE Mode	Ave. Freq., Hz	Exp. Mode	Ave. Freq., Hz
1	124.3	1	115.7
2	306.1	2	310.6
3	762.2	3	767.2
4	1089		
5	1116		
6	1488	4	1706
7	2015	5	2101
8	2157		
9	2368	6	2514
10	3274		

Experimental mode 4 is between the FE-predicted values for modes 6 and 7. Experimental mode 5 is between the FE-predicted values for modes 7 and 8. Lastly, experimental mode 6 is only about 6% higher than the FE-predicted value for mode 9. The apparent absence of some of the FE-predicted modes in the experimental spectrum is consistent with the known fact that the spatial load distribution used to excite the plate into vibration may not be able to excite all modes sufficiently to produce a readable peak in its frequency spectrum.

In sum, the computational results confirm the experimental conclusion that small to medium sized midplane delaminations in thick composite plates have a nearly negligible effect on the frequency spectrum in the range 0-4000 Hz. The computational results verify that existence of midplane delaminations would be difficult to detect by the free vibration method operating up to 4000 Hz.

Experimental spectra from quasi-isotropic plates with and without delaminations

Presented with the lack of effect of delaminations on the frequency spectra of unidirectional plates, we decided to fabricate plates of lower stiffness and to implant delaminations of greater severity. Lower stiffness was achieved by use of a quasi-isotropic stacking sequence for the composite. Greater severity in the delaminations was achieved by use of large, square pieces of Kapton release film, implanted at two levels between the midplane and the surface of the plate. The dimensions and delamination locations were shown earlier in Figure 5. Furthermore, in Plate No. 6-6-97, each delamination was composed of two pieces of Kapton film coated with mold release and stacked one on top of the other, whereas in Plate No. 5-27-97 each delamination was made of a single piece of Kapton film. The idea behind the double layer, mold-released delamination was to reduce friction between the two surfaces of the delamination, making them more free to move and affect the vibrational behavior.

The frequencies obtained from these two plates, with identical sizes and locations of delaminations, are presented in Table 8. The double layer of release film used for the

Table 8. Plate-to-Plate Comparison for Quasi-Isotropic Plates with Off-Midplane Delaminations (Ave. Freq. ± 1 Std. Dev.)

Edge-clamped configuration:

Plate No. 5-26-97	Plate No. 6-6-97
82.5 ± 1.2	85.6 ± 0.2
485.4 ± 8.1	489.9 ± 2.4
575.9 ± 2.1	582.3 ± 0.1
1156 ± 7.3	1157 ± 0.0
1324 ± 5.6	–
2088 ± 8.0	–

Unsupported configuration:

Plate No. 5-26-97	Plate No. 6-6-97
402.2 ± 0.2	413.0 ± 0.1
492.7 ± 0.1	504.9 ± 4.9
703.7 ± 8.4	705.2 ± 2.6
1262 ± 4.6	1273 ± 9.5
2078 ± 3.7	2029 ± 16.3
2466 ± 2.5	2429 ± 4.8

delaminations in Plate No. 6-6-97 made no apparent difference to the vibrational behavior.

More important results were obtained by cutting the square plates in half along the line shown in Figure 5. Thus, each plate was cut into an undelaminated half, designated by U, and a severely delaminated half, designated by D. The frequencies obtained from these rectangular plates are presented in Table 9. This table shows that, finally, an effect on the vibrational frequencies was produced; the frequencies for Plate 6-6-97-D, which contained the delaminations formed from double layers of film with mold release applied are shifted systematically downward with respect to those of all the other plates in this series. Single layer delaminations of the same size with no mold release (Plate No. 5-27-97-D) showed no effect on vibrational frequencies.

The results in Table 9 indicate that delaminations must be large, and the friction between the two faces of the delamination must be reduced, if the delaminations are to affect the plate's natural vibrational frequencies. However, reduction of friction between delamination faces is unrealistic for naturally occurring delaminations. This makes it very unlikely that naturally occurring delaminations, even if they were large, could be detected by the free vibration method.

In sum, to produce a noticeable, systematic downward shift in the natural frequencies of a plate, delaminations must be nearly half the area of the plate and their contacting surfaces must be friction free.

Table 9. Plate to Plate Comparison for Quasi-Isotropic Plates with and Without Delaminations (Ave. Freq. ± 1 Std. Dev.)

Edge-clamped configuration:

Plate No. 5-26-97-U	Plate No. 5-26-97-D	Plate No. 6-6-97-U	Plate No. 6-6-97-D
78.9 ± 0.1	79.8 ± 0.6	83.5 ± 0.3	84.4 ± 0.2
230.0 ± 7.1	238.9 ± 0.0	251.1 ± 0.4	253.9 ± 0.0
330.0 ± 4.1	338.0 ± 2.8	337.5 ± 9.6	320.2 ± 5.1
492.0 ± 0.2	494.8 ± 2.2	512.3 ± 0.1	479.2 ± 2.0
646.7 ± 2.9	653.8 ± 8.8	677.8 ± 0.5	647.5 ± 0.0
912.5 ± 5.0	921.3 ± 2.5	936.7 ± 4.9	872.6 ± 0.1
1062 ± 0.0	1042 ± 0.0	1107 ± 0.5	1033 ± 9.1
1354 ± 1.8	1364 ± 3.6	1399 ± 3.7	1325 ± 3.4
1927 ± 3.2	1950 ± 2.6	1983 ± 1.2	1963 ± 3.2
2552 ± 2.5	2575 ± 2.3	2599 ± 4.6	2433 ± 13.7
3669 ± 7.2	3683 ± 14.5	3736 ± 17.0	3439 ± 16.2

Unsupported configuration:

Plate No. 5-26-97-U	Plate No. 5-26-97-D	Plate No. 6-6-97-U	Plate No. 6-6-97-D
332.4 ± 0.0	387.5 ± 0.0	338.8 ± 3.2	335.7 ± 2.6
437.5 ± 0.0	437.4 ± 4.9	454.5 ± 2.5	452.3 ± 0.2
1203 ± 0.0	1217 ± 0.0	1242 ± 7.6	1241 ± 2.1
1318 ± 0.7	1321 ± 8.5	1370 ± 0.0	1357 ± 0.0
1818 ± 0.6	1843 ± 0.5	1881 ± 2.2	1834 ± 2.2
1990 ± 0.0	–	1977 ± 0.0	1933 ± 13.4
2091 ± 8.7	2060 ± 0.0	2054 ± 16.3	2052 ± 32.2
–	2131 ± 3.5	2159 ± 1.8	2146 ± 2.7
2363 ± 0.0	–	2426 ± 8.5	2298 ± 0.0
2833 ± 4.0	2875 ± 5.8	2878 ± 17.6	2851 ± 43.8
2983 ± 3.5	2950 ± 0.0	2953 ± 0.0	2932 ± 0.0
–	3045 ± 0.0	3061 ± 3.5	3048 ± 0.0

CONCLUSIONS

The findings and conclusions of the Phase I research project are summarized in this, the final, section.

- For best results, the piezoelectric patch sensors should be positioned on the plate surface as a pair at right angles to each other, i.e., parallel and perpendicular, respectively, to the edges of the plate. Frequency spectra from both sensors must be used for compiling a list of all the experimentally extracted frequencies of the vibrating plate.

- Both unsupported and edge-clamped configurations were simple to set up and yielded good spectra; either could be used. However, it must be remembered that because they impose different boundary conditions on the plate, the two support configurations led to different frequency spectra. Other support configurations, e.g. corner-clamping, are more difficult to set up and offer no advantages.

- Excitation by surface tap (near the center) and by edge tap both excited most major frequencies, but tended to give complementary amplitudes. Often, a frequency made barely perceptible after an edge tap would be clearly visible after a surface tap, and vice versa. This strongly suggests that spectra from both tap locations be collected.

- The random variation of the free vibration method itself, evaluated on any given plate, was small. For most peaks, the coefficient of variation (1 std. dev./mean) was under 1%. Plate-to-plate difference was usually only slightly greater, even given minor fabrication inconsistencies.

- Midplane delaminations in unidirectional thick plates did not cause the dramatic frequency shifts documented in the literature for unidirectional

thin plates with midplane delaminations.

- The computational results confirm the experimental conclusion that small to medium sized midplane delaminations in thick composite plates have a nearly negligible effect on the frequency spectrum in the range 0-4000 Hz. The computational results verify that existence of midplane delaminations would be difficult to detect by the free vibration method operating up to 4000 Hz.

- The kind of delaminations that begin to produce noticeable frequency shifts are those whose areas are nearly half that of the plate and whose free surfaces experience negligible frictional interaction.

In closing, we wish to emphasize that the geometric aspect of a plate that determines natural vibrational frequencies is relative dimension, such as length-to-thickness, not absolute dimension, such as thickness alone. Therefore, all the findings and conclusions in this report can be directly applied to thick composite structures whose length-to-thickness ratios are in the range 20-30. Delaminations would have a smaller effect on the frequency spectra of structures with length-to-thickness ratios lower than 20 (e.g., thicker-walled structures), and would have a greater effect on the spectra of structures with length-to-thickness ratios greater than 30.

REFERENCES

1. R.L. Ramkumar, "Compressive Fatigue Behavior of Composites in the Presence of Delaminations," in Damage in Composite Materials, ASTM-STP 775, K.L. Reifsnider, Ed., American Society for Testing and Materials, Philadelphia, 1982, pp. 184-210.

2. T.K. O'Brien, "Characterization of Delamination Onset and Growth in a Composite Laminate," in Damage in Composite Materials, ASTM-STP 775, K.L. Reifsnider, Ed., American Society for Testing and Materials, Philadelphia, 1982, pp. 140-167.

3. A.L. Highsmith and K.L. Reifsnider, "Stiffness Reduction Mechanisms in Composite Laminates," in Damage in Composite Materials, ASTM-STP 775, K.L. Reifsnider, Ed., American Society for Testing and Materials, Philadelphia, 1982, pp. 103-117.

4. J.W. Whitaker, W.D. Brosey, and M.A. Hamstad, "Correlation of Felicity Ratio and Strength Behavior of Impact-Damaged Spherical Composite Test Specimens," in Proc. Third Int. Symp. Acoustic Emission from Reinforced Composites, American Society for Nondestructive Testing, Columbus, OH, 1989.

5. N. Laws and G.J. Dvorak, "Stiffness Changes in Unidirectional Composites Caused by Crack Systems," Mechanics Mater., 2, 123-131 (1983).

6. G.J. Simitses and W.L. Yin, "Effect of Delamination on Axially Loaded Homogeneous Laminated Plates," AIAA J., 23, 1437-1444 (1985).

7. R. Talreja, "Transverse Cracking and Stiffness Reduction in Composite Laminates," J. Compos. Mater., 19, 355-375 (1985).

8. R. Talreja, "Stiffness Properties of Composite Laminates with Matrix Cracking and Interior Delamination," Engineering Fract. Mechanics, 25, 751-762 (1986).

9. Y.M. Han and H.T. Hahn, "Ply Cracking and Property Degradation of Symmetric Balanced Laminates under General In-Plane Loading," Compos. Sci. Technol., 35, 377-397 (1989).

10. Z. Tian and S.R. Swanson, "Residual Tensile Strength Prediction on a Ply-by-Ply Basis for Laminates Containing Impact Damage," J. Compos. Mater., 26, 1193-1206 (1992).

11. A.P. Christoforou and S.R. Swanson, "Strength Loss in Composite Cylinders under Impact," J. Engineering Mater. Technol., 110, 180-184 (1988).

12. P.A. Lagace and D.S. Cairns,"Tensile Response of Laminates to Implanted Delaminations," in Proc. 32nd International SAMPE Symposium and Exhibition, vol. 32, Society for the Advancement of Material Processing and Eng., Covina, CA, 1987, pp. 720-729.

13. M. Vikstrom, J. Backlund, and K.A. Olsson, "Nondestructive Testing of Sandwich Constructions Using Thermography," Composite Structures, 13, 49-65 (1989).

14. K. Reifsnider, E. Henneke, and W. Stinchcomb, "The Mechanics of Vibrothermography," in Mechanics of Nondestructive Testing, W. Stinchcomb, Ed., Plenum Press, New York, pp. 249-276 (1980).

15. J.J. Tracy and G.C. Pardoen, "Effect of Delamination on the Natural Frequencies of Composite Laminates," J. Compos. Mater., 23, 1200-1215 (1989).

16. W.H. Tsai and J.C.S. Yang, "Nondestructive Evaluation of Composite Structures Using System Identification Technique," J. Eng. Mater. Technol., 110, 134-139 (1988).

17. J.E. Grady and E.H. Meyn, "Vibration Testing of Impact-Damaged Composite Laminates," Proc. AIAA/ASME/ASCE/AHS/ASC 30th Structures, Struct. Dynamics, and Mater. Conf., AIAA, Washington, DC, 1989, pp. 2186-2193.

18. M.D. Shelby, H.J. Tai, and B.Z. Jang, "Vibration Based Non-Destructive Evaluation of Polymer Composites," Polym. Eng. Sci., 31, 47-55 (1991).

19. M.H. Shen and J.E. Grady, "Free Vibrations of Delaminated Beams," AIAA J., 30, 1361-1370 (1992).

20. L.H. Tenek, E.G. Henneke, and M.D. Gunzburger, "Vibration of Delaminated Composite Plates and Some Applications to Non-Destructive Testing," Composite Structures, 23, 253-262 (1993).

21. X.H.Jian, H.S. Tzou, C.J. Lissenden, and L.S. Penn, "Damage Detection by Piezoelectric Patches in a Free Vibration Method," J. Compos. Mater., 345-359 (1997).

22. H.S. Tzou, "Integrated Distributed Sensing and Active Vibration Suppression of Flexible Manipulators Using Distributed Piezoelectrics," J. Robot. Syst., 6, 745-767 (1989).

23. H.S. Tzou, "Distributed Modal Identification and Vibration Control of Continua: Theory and Applications," ASME J. Dyn. Syst., Meas. and Contr., 113, 494-499 (1991).

24. Product Data Sheet, AMP Inc., Norristown, PA, 1997.

25. E.L. Wilson and A. Ibrahimbegovic, "Use of Incompatible Displacement Modes for the Element Stiffness and Stresses," Finite Elements in Analysis and Design, 7, 229-241 (1990).

26. Computers and Structures, Inc. (1996), SAP2000N - Integrated Finite Element Analysis and Design of Structures, V 6.02.

27. P.S. Frederiksen, "Experimental Procedure and Results for the Identification of Elastic Constants of Thick Orthotropic Plates," J. Compos. Mater., 31, 360-382 (1997).

APPENDIX A

Thickness Maps of Laminated Plates

Plate No. 1-29-97

V_f=0.43

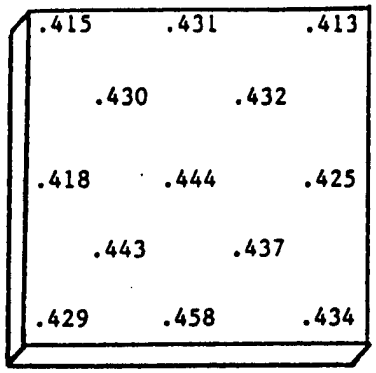

Plate No. 2-13-97

V_f=0.42

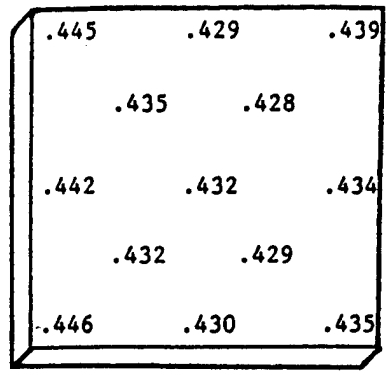

Plate No. 3-6-97

V_f=0.48

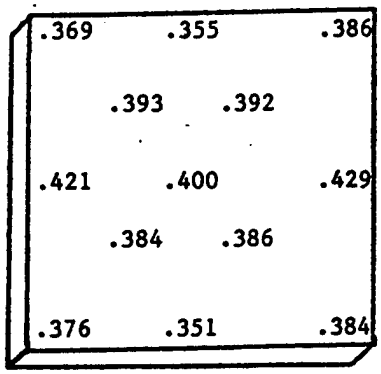

Plate No. 3-7-97

V_f=0.48

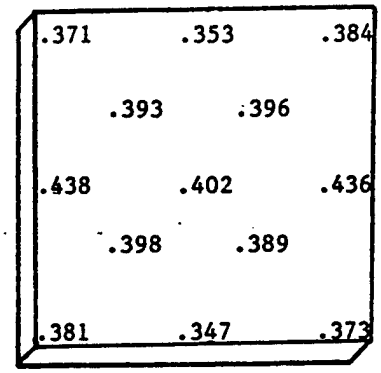

Plate No. 5-26-97

V_f=0.56

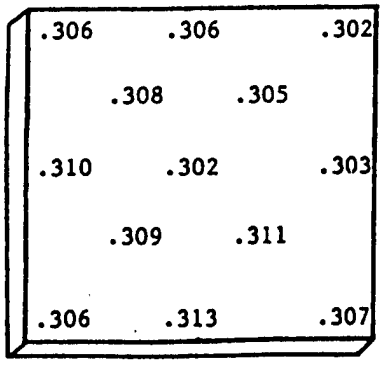

Plate No. 6-6-97

V_f=0.56